Improved Subcarrier Selection Technique for Power Line Communications

Babatunde Segun Adejumobi*, Thokozani Shongwe, and Ali N. Hasan

Department of Electrical and Electronic Engineering Technology, Johannesburg 2028, South Africa; Email: tshongwe@uj.ac.za; alinabeal1981@gmail.com
*Correspondence: bsaadejumobi@uj.ac.za

***Abstract*—This paper proposes Power Line Communication (PLC) schemes that improve the data rate of PLC systems while combating impairments resulting from frequency disturbances like impulse noise. Firstly, a modified subcarrier selection technique that can be employed to transmit one or more M-ary Phase-Shift Keying (MPSK) or M-ary Quadrature Amplitude Modulated (MQAM) symbols within a subset of the subcarriers of an orthogonal frequency division multiplexing symbol. The proposed subcarrier selection technique employs the cyclic rotation of a set of subcarriers, chosen from a group of subcarriers to transmit the selected MPSK or MQAM symbols. A second scheme that employs the rotation of MPSK or MQAM symbols among a group of subcarriers, to increase the data rate of the PLC system is proposed. The proposed schemes show improvement in error performance when tested over Additive White Gaussian Noise (AWGN) and impulse noise of a PLC system despite the increase in the data rate.**

***Keywords*—Subcarrier selection, subcarrier allocation, Orthogonal Frequency Division Multiplexing (OFDM), power line communication, quadrature amplitude modulation, impulse noise**

I. Introduction

Power Line Communication (PLC) systems have been employed for different purposes for a very long time. Some of their applications include telephony, control of street lights, intercoms, power transmission systems, and smart grids [1]. PLC is a convenient and cost-effective communication system, this is because power distribution networks are available in almost every community [2]. PLC has become all the more attractive because of its application in the Internet of Things (IoT) for smart grid applications [3]. In order to realize seamless communication among home appliances and across the grid, small and reliable power line modems have been designed having different standards emerging since 1990s [4]. Some of the standards which have emerged over time include the HomePlug AV [4, 5], HomePlug 1.0 [6], HomePlug AV2 [7], etc. Despite the numerous advantages of PLC, it is always limited due to noise disturbances along its channel.

Manuscript received May 10, 2022; revised December 10, 2022; accepted January 10, 2023.

Hence, researchers are constantly looking for options to mitigate the noise effect in PLC [8].

An important modulation technique that has been found to be very attractive for PLC systems is Orthogonal Frequency Division Multiplexing (OFDM), this is because of its ability to mitigate intersymbol interference and interchannel interference. Furthermore, it offers improved spectral and power efficiency and is immune to multipath fading [9, 10]. A pictorial representation of the subcarrier frequencies of an OFDM symbol is presented in Fig. 1, while the system model of an OFDM transmission system as presented in [11], is shown in Fig. 2.

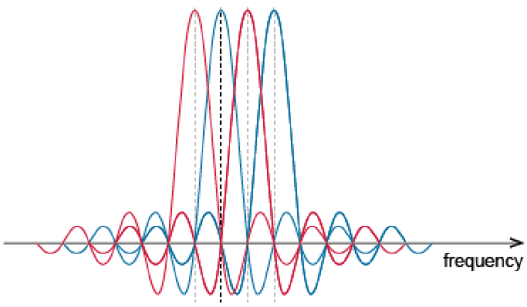

Figure 1. Multiple OFDM subcarrier frequencies

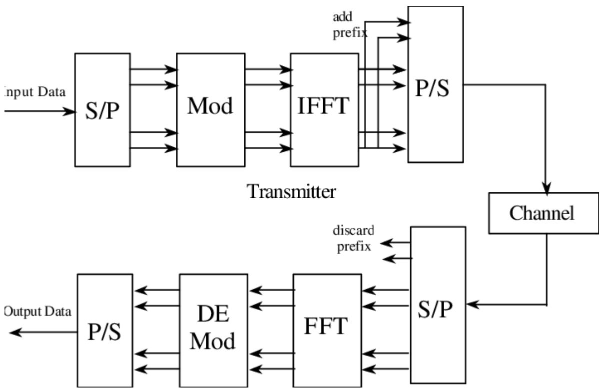

Figure 2. System model of an OFDM transmission scheme [11]

The numerous advantages of OFDM to communication systems, in general, have engendered more focus by researchers of PLC to seek more applications of OFDM to PLC systems including improvements in spectral efficiency of PLCs [12].

doi:10.12720/jcm.18.2.123-128

II. Related Works

The OFDM scheme is an attractive scheme for PLC systems because of its ability to combat noise distortions along the PLC channels. This noise distortion is evident because PLC systems employ power distribution networks for communication [13]. For example, the authors in [12] showed that employing quadrature phase-shift keying (QPSK) with OFDM is capable of combating frequency disturbances when selected subcarriers are used for transmission. Furthermore, in the research presented in [13], the authors proposed different selected subcarrier techniques, where one or two M-ary PSK (MPSK) symbols are transmitted over some selected subcarriers. Furthermore, in [14], the authors presented the effect of asynchronous noise and its performance On PLC when used with OFDM.

In similar research, the authors in [15] presented a robust transmission OFDM M-ary frequency-shift keying (OFDM-MFSK) scheme that is capable of performing better in fast fading channels. Firstly, this OFDM-MFSK scheme groups the OFDM symbol into ψ groups, such that the OFDM symbol is given as $\boldsymbol{X} = [\boldsymbol{x}_1 \quad \boldsymbol{x}_2 \quad \cdots \quad \boldsymbol{x}_\psi]$, with each of the groups $\boldsymbol{x}_i = [x_1 \quad x_2 \quad \cdots \quad x_\ell]$, for $i \in [1{:}\,\ell]$ having ℓ subcarriers. This means the fast Fourier transform (FFT) size of the OFDM symbol becomes $\psi\ell$. In each of the i-th groups, only one subcarrier is active while others are inactive. Although this scheme exhibits improved performance in fast fading channels, does not need prior knowledge of channel estimates, and is robust against time variation, it was not tested with the QPSK modulation and had more room for improvements in terms of data rate because of the low bandwidth efficiency of about 0.5 per subcarrier.

Having identified these lapses, the authors in [12] proposed several schemes to improve the data rates. The increased data rate was achieved by employing at most three subcarriers to transmit QPSK symbols for the selected subcarriers. For example, the conventional QPSK-OFDM system, where all subcarriers are enabled for transmission is Scheme A. Scheme B is similar to the OFDM-MFSK described earlier. However, instead of just transmitting a tone on the selected subcarrier of the individual groups, a QPSK symbol is transmitted.

In Scheme C, the authors employed a quadrature indexing technique similar to but not exactly the method of quadrature spatial modulation OFDM given in [16]. This is because the method of [16] was employed with a multiple-input multiple-output (MIMO) wireless system having several antennas. The real part and the imaginary part of the QPSK symbol are transmitted through different subcarriers. For example, given that the QPSK symbol $x = x_r + jy_i$ is selected for transmission by the first and third subcarrier. If we assume that $\ell = 4$, then, for Scheme C, $\boldsymbol{x}_i$ will become $\boldsymbol{x}_i = [x_r \quad 0 \quad jy_i \quad 0]$, where x_r and y_i are the real and imaginary parts, respectively, of the QPSK symbol x, while $j = \sqrt{-1}$. This scheme showed that the data rate of PLC can be improved while combating the different noises, viz, Additive White Gaussian Noise (AWGN), narrowband noise [17], and impulse noise [18, 19]. Although this scheme has shown improvement in data rate, we have noted that it did not consider the performance of Quadrature Amplitude Modulation (QAM). Furthermore, we note that there is still room for improvement in the data rate. Hence, we are motivated to propose enhanced subcarrier selection techniques that are capable of increasing the throughput of PLC communication systems while retaining the link quality of the PLC system.

Based on the points mentioned above, we are the first contribution of this paper is to present the BER performance of an M-ary QAM (MQAM) subcarrier selection scheme for an OFDM PLC system. Secondly, we propose an improved subcarrier selection scheme capable of improving the data rate of PLC systems. The proposed scheme employs sets of cyclically rotated MQAM symbols to improve the data rate of PLC systems.

Notations: We have employed the following notations in this paper; matrices are denoted by bold uppercase letters, while bold lowercase letters denote vectors unless it is stated otherwise. The notations $(\cdot)^T$ and $\|\cdot\|_F$ represent the transpose and Frobenius norm, respectively. $j = \sqrt{-1}$ is a complex number while $\lfloor z \rfloor_{2p}$ represents the nearest power of 2 less than equal to z.

III. System Model

A. Background of Subcarrier Selection

The input bits of a PLC system that are to be transmitted through the PLC channel is employed to select tones of a Multiple Frequency-Shift Keying (MFSK) modulation or a symbol of an M-ary amplitude and/or phase modulation (APM) symbol. To prevent intersymbol interference, OFDM, a multi-carrier modulation system, where the information to be transmitted is carried by N subcarrier frequencies which are orthogonal to one another is employed [20]. Traditionally, the conventional time-domain OFDM symbol is of the form.

$$\boldsymbol{x} = [x_1 \quad x_2 \quad \cdots \quad x_N]^T \tag{1}$$

The OFDM symbol of the α-th data to be transmitted is obtained by performing the inverse fast Fourier on the input vector $\boldsymbol{x}$ given by [21]:

$$x_k = \frac{1}{\sqrt{N}} \sum_{\alpha=0}^{N-1} \boldsymbol{x}_\alpha e^{\frac{j2\pi k\alpha}{N}} \tag{2}$$

where x_k is the k-th IFFT of the input vector $\boldsymbol{x}$. $\boldsymbol{x}_\alpha$ is the α-th element of the input vector $\boldsymbol{x}$. N is the IFFT size of the OFDM modulator.

To transmit APM symbols within a block of ℓ subcarriers, the frequency selection technique splits the input bits meant for this purpose into two parts. One set of the input bits is employed to select one or more subcarriers that are used for the transmission of the APM symbols. The other set of bits is employed to select the APM symbols to be transmitted. However, this is not all, as there may be a need for further processing. For example, given that within a block of four subcarriers only one subcarrier is intended for transmitting a BPSK symbol. There will be a need for $\log_2 \ell = \log_2 4 = 2$ bits to select the subcarrier, while another $\log_2 M = \log_2 2 = 1$ bit to select the BPSK symbol to be transmitted, viz. -1 or $+1$. If we assume that the input bits are (010), the assignments will be as given in the first row of Table I.

TABLE I: APM AND SUBCARRIER SELECTION METHOD

Input bits	Subcarrier bits	Index	APM bits	symbol
010	01	2	0	-1
111	11	4	1	+1

If we assume that two subcarriers will be employed for the PLC transmission scheme, then, the input bits for selecting transmit subcarrier in Table I can be redesigned, such that bit assignment for the subcarriers within a given block of subcarriers of $\ell = 4$ takes the form given in Table II [12].

TABLE II: BIT ALLOCATION FOR TWO SUBCARRIER SELECTION

Input bits	Index
00	1,2
01	3,4
10	2,3
11	1,4

B. *Proposed System Model for PLC Subcarrier Selection*

1) *Rotated subcarrier technique (S_1)*

The proposed subcarrier selection technique improves on the technique given in [12] by employing cyclically rotated APM symbols to improve the data rate. We present the subcarrier selection in the form of codewords and codebooks.

The proposed subcarrier selection technique improves on the technique given in [12] by employing cyclically rotated APM symbols to improve the data rate. We present the subcarrier selection in the form of codewords and codebooks [22].

Codebook 1	➔	1,2	2,3	3,4	4,1	
Codebook 2	➔	1,3	2,4	3,1	4,2	(3)
Codebook 3	➔	1,4	2,1	3,2	4,3	

TABLE III: CODEBOOK DESIGN FOR SUBCARRIERS

Codebook	Subcarrier	Used/ Unused	Codebook matrix
Codebook 1	1,2	used	$[s_1 \quad s_2 \quad 0 \quad 0]^T$
	2,3	used	$[0 \quad s_1 \quad s_2 \quad 0]^T e^{j\theta_1}$
	3,4	used	$[0 \quad 0 \quad s_1 \quad s_2]^T e^{j\theta_2}$
	4,1	used	$[s_2 \quad 0 \quad 0 \quad s_1]^T e^{j\theta_3}$
Codebook 2	1,3	unused	$[s_1 \quad 0 \quad s_2 \quad 0]^T$
	2,4	unused	$[0 \quad s_1 \quad 0 \quad s_2]^T$
	3,1	unused	$[s_2 \quad 0 \quad s_1 \quad 0]^T$
	4,2	unused	$[0 \quad s_2 \quad 0 \quad s_1]^T$
Codebook 3	1,4	used	$[s_1 \quad 0 \quad 0 \quad s_2]^T e^{j\theta_4}$
	2,1	used	$[s_2 \quad s_1 \quad 0 \quad 0]^T e^{j\theta_5}$
	3,2	used	$[0 \quad s_2 \quad s_1 \quad 0]^T e^{j\theta_6}$
	4,3	used	$[0 \quad 0 \quad s_2 \quad s_1]^T e^{j\theta_7}$

If we assume that the selected symbols for the two selected subcarriers are s_1 and s_2, where s_i, for $i \in [1:2]$ is a symbol of an M-ary APM constellation $\boldsymbol{\chi} = [s_1, \cdots, s_M]$, where M is the constellation size of $\boldsymbol{\chi}$. Then, the output vectors based on the cyclic subcarrier arrangement is as presented in Table III.

In Table III, θ_i is defined as:

$$\theta_i = \frac{(i-1)\pi}{8} \tag{4}$$

where $i \in$ [1:8].

Based on the subcarrier arrangement given in Eq. (3), the number of subcarrier combinations possible, given that two subcarriers are selected for communication out of the ℓ subcarriers within a block is $\ell(\ell-1)$. Whereas the number of bits per subcarrier group for the subcarrier selection scheme in [12] is $R_{old} = b + \log_2 L_{old}$ bits, where $\text{b} = 2\log_2 M$ and $L_{old} = \left\lfloor \frac{\ell(\ell-1)}{2} \right\rfloor_{2p}$. The number of bits that can be achieved using the proposed method is given as:

$$R_{new} = 2\log_2 M + \log_2 \left(\left\lfloor \frac{\ell(\ell-1)}{2} \right\rfloor_{2p} \right) \tag{5}$$

For example, given that the number of subcarriers within a group to be employed is $\ell = 4$ and that the M-ary QAM (MQAM) scheme that is employed is 4QAM. The number of bits for $R_{old} = 2\log_2 4 + \log_2 4 = 4 + 2 = 6$. However, the number of bits per subcarrier group for the proposed scheme is $R_{S_1} = 2\log_2 4 + \log_2 8 = 4 + 3 = 7$. This improvement is significant because the number of bits gained is proportional to the number of blocks that exist within a single OFDM block. For example, if an OFDM symbol has a size of $N = 256$, the number of bits gained b_{gain} by transmitting the OFDM symbol over a PLC channel can be given as:

$$b_{gain} = \frac{N(R_{new} - R_{old})}{\ell} \tag{6}$$

2) *Rotated symbol technique (S_2)*

TABLE IV: ROTATED SYMBOL TECHNIQUE FOR $\binom{\ell}{k}$ SUBCARRIER SELECTION

Input bits	Selected subcarrier	$k = 2$ rotation multiplier
00	1,2	1,1
01	3,4	$1, e^{j\theta}$
10	2,3	$e^{j\theta}, 1$
11	1,4	$e^{j\theta}, e^{j\theta}$

This method enhances the data rate by selectively and temporally rotating the symbols of the selected subcarriers. A major advantage of this method is that it can be employed on pre-existing subcarrier selection techniques to improve the data rate. Furthermore, this method increases the data rate based on the number of selected subcarriers needed for transmission within a given OFDM subcarrier block. For example, if the number of selected subcarriers within an OFDM subgroup is $k = 2$, the number of extra bits that are required for the transmission when compared to the conventional technique is 2 bits. The rotation of symbols for a block of four subcarriers having two selected subcarriers is presented in Table IV.

Given that the symbol rotation technique is applied to the subcarrier selection scheme with $M = 4$, $k = 2$, and $\ell = 4$, the number of bits per subcarrier group is given as:

$$R_{S_2} = 2\log_2 M + \log_2\left(\left\lfloor \frac{\ell(\ell-1)}{2} \right\rfloor_{2p}\right) + k \qquad (7)$$

where M is the constellation size of the APM symbol employed and ℓ is the subcarrier block size. Whereas the number of bits for R_{old} is 6 bits when 4QAM is employed, and the number of subcarriers for each subgroup is 4, whereas the number of bits for Scheme S_2 is 8, 2 bits are employed to select the two subcarriers needed for transmitting two MQAM symbols, 4 bits are employed to select the two MQAM symbols and an additional 2 bits to select the subcarrier rotation for the respective symbols as given in Table IV. As an example, assume that the bit stream 10101101 is to be transmitted using this scheme, the first 2 bits "10" will be used to select subcarriers 1,4 as given in Table II. The next four bits 10 11 will be employed to select two MQAM symbols x_1 and x_2 for $x_\zeta \in [x_1 \cdots x_M]$. The remaining 2 bits 01 will be employed to select the rotation $1, e^{j\theta}$ presented in Table IV which is then used to multiply the symbols x_1 and x_2, respectively. In summary, the symbol x_1 will be transmitted on subcarrier 1, while $x_2 e^{j\theta}$ will be transmitted in subcarrier 4.

IV. Simulation Results and Discussion

This section presents the simulation results of the proposed schemes S_1 and S_2. Furthermore, the results for S_2 are compared with the results of a similar scheme in [12]. However, for the results of S_1 we made an unfair comparison since the data rate per subcarrier group will always be 1 bit greater than R_{old} [12]. For the different figures, we have used the notation (S_i, R_{S_i}, MQAM) for $i \in [1{:}2]$, to indicate the application of additive white Gaussian noise (AWGN) only. In some instances, where the simulation involves the inclusion of impulse noise together with AWGN in the simulation, we have used the notation (S_i, R_{S_i}, MQAM, IM). The property of impulse noise employed for the simulation is the Gilbert-Elliot model having parameters as defined in [12].

Fig. 3 shows the plots for the proposed Scheme S_1, an which offers improved data rate by employing the rotated subcarrier technique. Although the error performance is unfairly compared with [1] due to the different spectral lengths, we have included both plots. This is necessary so that the bit-error rate performance is viewed in partial comparison with the pre-existing scheme. From the plots shown in Fig. 3, we find out that like the S_{old} scheme, the S_1 scheme exhibits an improved bit-error-rate performance for AWGN when the signal-to-noise ratio $\frac{E_S}{N_o}$ is less than 10 dB. For example, the S_1 scheme can achieve an average bit-error probability of 10^{-5} when 4-QAM modulation is applied under AWGN when the signal-to-noise ratio is 9.5 dB. However, to achieve the same average bit-error probability of 10^{-5} in the presence of AWGN and impulse noise, the S_1 scheme will require 27.5 dB using the same modulation of 4-QAM. For $R_{S_1} = 11$ bits per subcarrier group with 16QAM modulation, the S_1 scheme can achieve an average bit-error probability of 10^{-5} with a signal-to-noise 18 dB for AWGN. For the $R_{S_1} = 11$, $M = 16$ with AWGN and impulse noise, the 10^{-5} average bit-error probability is achieved by a signal-to-noise ratio of 31 dB. Comparing the plots for Scheme S_1 and S_{old} under AWGN and impulse noise, it can be seen that there is an improvement of at least ≈ 1 dB gain by the S_1 over the corresponding S_{old} schemes.

Considering Fig. 4, which presents plots for the rotated symbol scheme S_2. The plots for the S_2 and S_{old} schemes give a fair comparison of the two schemes since the data rate being compared is the same. The performance of the S_{old} and S_1 techniques seem to show similar performance for $R_{S_2} = R_{old} = 6$ bits per subcarrier group having only AWGN at the receiver.

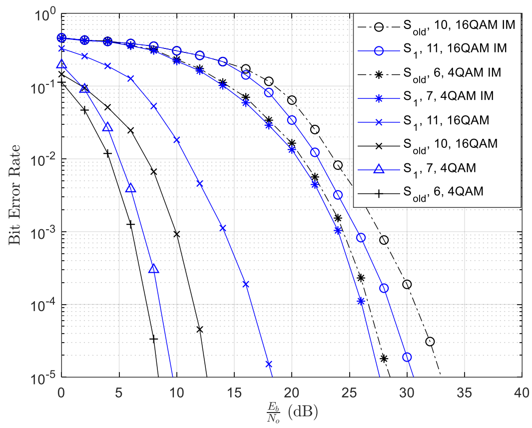

Figure 3. BER Performance for PLC Schemes with $P_{gb} = 0.1$, $P_{bg} = 0.9$, $T = 10^{-2}$, $k = 1$ and $h = 0.5$ (S_{old} and S_1)

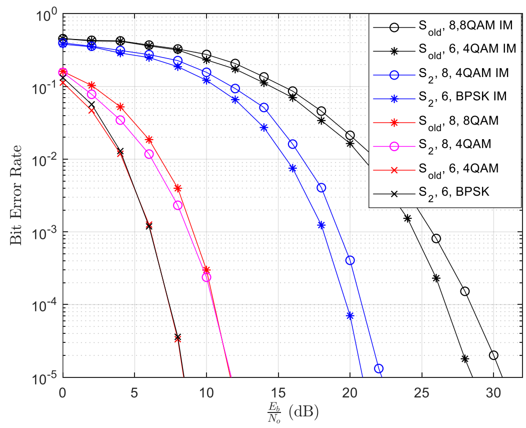

Figure 4. BER Performance for PLC Schemes with $P_{gb} = 0.1$, $P_{bg} = 0.9$, $T = 10^{-2}$, $k = 1$ and $h = 0.5$ (S_{old} and S_2)

For example, at a signal-to-noise ratio of 8 dB, both schemes can attain an average bit-error probability of 10^{-5}.

However, a slightly different trend is presented by the plots for $R_{S_2} = R_{old} = 8$.

The S_2 plots show superior performance when the signal-to-noise ratio is between 2 and 10 dB. However, at $\frac{E_S}{N_o} > 10$ dB, the plots demonstrate similar performance. For instance, the S_2 scheme achieved ≈ 1 dB gain at an average bit-error probability of 4×10^{-3}, however, both schemes achieved an average bit-error probability of 10^{-5} when the signal-to-noise ratio is ≈ 12 dB. Referring to the simulation plots which combine the PLC noise (impulse noise and AWGN), the plots demonstrate that for $R_{S_2} = 6$ and $R_{S_2} = 8$, the S_2 scheme was able to achieve an average bit-error probability 10^{-5} when the signal-to-noise ratio is ≈ 21 and 22 dB, respectively. However, in comparison with their S_{old} counterpart, it is observed that the S_2 scheme has a superior performance of at least 7 dB gain over the $R_{S_{old}} = 6$ and $R_{S_{old}} = 8$. Furthermore, comparing the two schemes i.e., S_1 and S_2, it is quite evident that the S_2 scheme has a robust performance in dealing with impulse noise. This is supported by the fact that, even at a higher data rate of $R_{S_2} = 8$, the S_2 technique requires only a maximum of 22 dB in signal-to-noise ratio to achieve an average bit-error probability of 10^{-5} while Scheme S_1 require 27.5 dB to attain an average bit-error probability of 10^{-5} when $R_{S_1} = 7$, a data rate which is less than R_{S_2}.

V. Conclusion

This paper presented two techniques for improving the data rate of PLC systems, viz: subcarrier rotation and symbol rotation techniques. Depending on the method used, the techniques can increase the data rate and combat effectively AWGN and PLC's impulse noise. Of the two techniques presented in this paper, the S_2 scheme demonstrated the most encouraging results in terms of increased data rate and improved signal-to-noise ratio gain which is greater than 7 dB in the presence of AWGN impulse noise. The significance of this is that a large amount of bits can be transmitted using the same bandwidth. However, if the desire is to maintain quality of service, then, employing low-order QAM will offer BER.

VI. Future Work

The current work focused on the improvement of the spectral efficiency of PLC systems using different techniques, in the future, areas such as low computational complexity detectors for PLC systems would be very important as the popular maximum-likelihood detector consumes a lot of processing resources like the processor or power consumption. Furthermore, the application of AI in many engineering problems has changed the engineering sphere in many areas. More recently, the application of machine learning or deep learning to detect transmitted symbols has been applied in many areas of wireless communication. In the future, the aspect of deep learning and machine learning can be applied to this aspect of PLC to improve the various detection techniques.

Conflict of Interest

The authors declare no conflict of interest.

Author Contributions

Conceptualization of idea by Thokozani and Babatunde, Supervision of the work by Thokozani and Ali.

Acknowledgment

The authors would like to appreciate the University of Johannesburg for the funding and facilities made available for this research.

References

[1] K. Bernacki, D. Wybránczyk, M. Zygmanowski, A. Latko, J. Michalak, and Z. Rymarski, "Disturbance and signal filter for powerline communication," *Electronics*, vol. 8, no. 4, p. 378, Mar 2019.

[2] C. Xilin, C. Rui, and Y. Liuqing, "Relay-aided amplify-and-forward powerline communications," in *Proc. IEEE Transactions on Smart Grid*, vol. 4, no. 1, pp. 265–272, 2013.

[3] Stuckenberg and H. Blume, "A hardware efficient preamble detection algorithm for powerline communication," *Journal of Communications*, vol. 13, no. 1, pp. 1-7, 2018.

[4] H. A. Latchman, S. Katar, L. Yonge, and S. Gavette, *Home Plug AV and IEEE 1901: A Handbook for PLC Designers and Users*, 1st ed., New Jersey, Wiley-IEEE Press, 2013, ch. 4, pp. 37-40.

[5] Home Plug AV2 Technology, Home Plug Alliance Standard, 2010.

[6] Home Plug 1.0 Specification, Home Plug Alliance Standard, Version 1.0.1, 2001.

[7] Home Plug AV2 Technology, Home Plug Alliance Standard, 2010.

[8] O. Kolade, A. M. Abu-Mahfouz, and L. Cheng, "A subcarrier permutation scheme for noise mitigation and multi-access in powerline channels," in *Proc. IEEE International Symposium on Power Line Communications and Its Applications*, 2021, pp. 19-24.

[9] M. Khan, S. Iqbal, and W. Asghar, "A review paper on: The PAPR analysis of orthogonal frequency division multiplexing (OFDM)," *International Journal of Mobile Network Communications & Telematics*, vol. 4, no. 1, Feb. 2014.

[10] M. I. Youssef, A. E. Emam, and M. Abd Elghany, "ICI and PAPR enhancement in MIMO-OFDM system using RNS coding," *Journal of Communications*, vol. 14, no. 7, pp. 629-635, 2019.

[11] X. Ma, H. Kobayashi, and S. C. Schwartz, "An EM-based estimation of OFDM signals," in *Proc. IEEE Wireless Communications and Networking Conference Record*, 2002, pp. 228-232.

[12] V. N. Papilaya, T. Shongwe, A. J. H. Vinck, and H. C. Ferreira, "Selected subcarriers QPSK-OFDM transmission schemes to combat frequency disturbances," in *Proc. IEEE International Symposium on Power Line Communications and Its Applications*, 2012, pp. 200–205.

[13] N. Pavlidou, A. J. H. Vinck, J. Yazdani, and B. Honary, "Power line communications: state of the art and future trends," *IEEE Communications Magazine*, vol. 41, no. 4, pp. 34–40, 2003.

[14] S. Jagannathan, A. Morales, and S. Agili, "Performance of OFDM-based power line communication under asynchronous noise," in *Proc. IEEE International Conference on Consumer Electronics*, 2014, pp. 371–372.

[15] M. Wetz, W. G. Teich, and J. Lindner, "OFDM-MFSK with differentially encoded phases for robust transmission over fast fading channels," in *Proc. 11th International OFDM-Workshop*, 2006.

[16] B. S. Adejumobi and N. Pillay, "Quadrature spatial modulation orthogonal frequency division multiplexing," *Journal of Telecommunication, Electronic and Computer Engineering*, vol. 10, no. 4, pp. 51–57, 2018.

[17] M. Katayama, T. Yamazato, and H. Okada, "A mathematical model of noise in narrowband power line communication systems," *IEEE*

Journal on Selected areas in Communications, vol. 24, no. 7, pp. 1267–1276, 2006.

[18] T. Shongwe, A. H. Vinck, and H. C. Ferreira, "The effects of periodic impulsive noise on OFDM," in *Proc. IEEE International Symposium on Power Line Communications and Its Applications*, IEEE, 2015, pp. 189–194.

[19] T. Shongwe, A. H. Vinck, and H. C. Ferreira, "A study on impulse noise and its models," *SAIEE Africa Research Journal*, vol. 106, no. 3, pp. 119–131, 2015.

[20] B. S. Adejumobi, "Index modulation for next generation wireless communications." Ph.D. dissertation, University of KwaZulu-Natal, Durban, South-Africa, 2018.

[21] Y. S. Cho, J. Kim, W. Y. Yang, and C. G. Kang, *MIMO-OFDM Wireless Communications with MATLAB*, John Wiley & Sons, 2010.

[22] B. S. Adejumobi and N. Pillay, "Low-Complexity detection for space-time block coded spatial modulation with cyclic structure," *Journal of Communications*, vol. 13, no. 7, pp. 391-395, 2018.

Babatunde Segun Adejumobi received the B.Sc. and M.Sc. degrees in electronic and computer engineering from Lagos State University, Lagos, Nigeria, in 2007 and 2012, respectively, and the Ph.D. degree in electronic engineering (wireless communication) from the Department of Electrical, Electronic, and Computer Engineering, University of KwaZulu-Natal, Durban, South Africa. His current research includes spatial modulation, space-time block-coded modulation, and orthogonal frequency division multiplexing. However, he also has an interest in optical communication, wireless communications, image processing, and power line communications.

Thokozani Shongwe received the B.Eng. degree in electronic engineering from the University of Swaziland, Swaziland, in 2004, and the M.Eng. degree in telecommunications engineering from the University of the Witwatersrand, South Africa, in 2006, and the D.Eng. degree from the University of Johannesburg, South Africa, in 2014. He is currently an Associate Professor with the Department of Electrical and Electronic Engineering Technology, University of Johannesburg. He was a recipient of the 2014 University of Johannesburg Global Excellence Stature (GES) Award, which was awarded to him to carry out his postdoctoral research at the University of Johannesburg. In 2016, he was a recipient of the TWAS-DFG Cooperation Visits Program funding to do research in Germany. Other awards that he has received in the past are: the Post-Graduate Merit Award scholarship to pursue his master's degree at the University of the Witwatersrand, in 2005, which is awarded on a merit basis. In the year 2012, he (and his co-authors) received an Award of the Best Student Paper at the IEEE ISPLC 2012 (power line communications conference) in Beijing, China. His research fields are in digital communications and error correcting coding. His research interests include power-line communications, cognitive radio, smart grid, and visible light communications.

Ali N. Hasan received his B.Eng. in Electrical and Electronic Engineering from the Hashemite University in Jordan in 2005. Dr. Hasan completed his M. Eng. in Electrical Engineering from North West University in 2010 and his D.Eng. (PhD) degree in Electrical and Electronic Engineering in the year 2014 from University of Johannesburg in South Africa respectively. Dr. Hasan served as a senior lecturer for six years in the electrical engineering department- University of Johannesburg. He is currently an Assistant professor at the department of electrical engineering at the Higher Colleges of Technology in Abu Dhabi, UAE. Dr. Hasan research work mainly focuses on the applications of Artificial Intelligence applications in energy and renewable energy, Power systems and Noise mitigation. Dr. Hasan has published more than 60 papers in international conferences and journals and supervised several masters and PhD students.